Available online at www.sciencedirect.com
SCIENCE DIRECT®
Engineering Structures 26 (2004) 543–551
ENGINEERING STRUCTURES
www.elsevier.com/locate/engstruct

Seismic design of low-rise steel frames with buckling-restrained braces

Jinkoo Kim *, Youngil Seo

Department of Architectural Engineering, Sungkyunkwan University, Suwon 440 746, South Korea

Received 26 January 2003; received in revised form 27 October 2003; accepted 11 November 2003

Abstract

In this study, a direct displacement design procedure for steel frames with buckling-restrained braces (BRBs) is presented. The proposed structure system is composed of a hinge-connected main structure, which is designed to remain elastic under seismic load, and BRBs resisting all lateral loads. At seismic event, the BRBs dissipate dynamic energy through stable hysteretic behavior. A displacement-based seismic design procedure is applied to model structures to check the applicability of the design procedure. Two artificial earthquake records are generated from a design spectrum, and the response spectra constructed based on the earthquake records are utilized in the design process. Time-history analyses are carried out to confirm that the maximum displacements coincide with the target displacements. The results show that the seismic performance of the 3- and 5-story model structures designed in accordance with the proposed method coincide well with the given design objectives.

Keywords: Seismic design; Buckling-restrained braces; Direct displacement-based design; Steel frames

1. Introduction

The conventional philosophy of seismic design depends on inelastic deformation of structural members for dissipation of input earthquake energy. This design concept may provide safety and economy in seismic design, but may not prevent damages in structures after being shaken by an earthquake. The damage in main structural members can be prevented or minimized by connecting beams and columns with hinges, and employing lateral-load resisting members to withstand lateral seismic load [1]. In this so-called a damage-tolerant braced frame (DTBF), most of the energy dissipation and structural damages caused by an earthquake will be concentrated on the lateral-load resisting members, and the main members will remain elastic. After earthquake, the damaged lateral-load resisting members can be replaced easily at reasonable cost.

Generally, steel braces are used as an economic means of providing lateral stiffness to a steel structure. However, the energy dissipation capacity of a steel braced structure subjected to earthquake loads is limited due to the buckling of the braces. This is the main reason for most seismic design provisions to regulate lower value for the response modification factor to a braced frame than to a moment frame. The energy dissipation or damage prevention capacity of a steel framed structure can be greatly enhanced by employing buckling-restrained braces (BRBs). They usually consist of a steel core capable of undergoing significant inelastic deformation and a casing for restraining global and local buckling of the core element. According to previous research [2–5], an BRB exhibits stable hysteretic behavior with high-energy dissipation capacity. The use of BRBs greatly enhances the energy dissipation capacity of the structure and decreases the demand for inelastic deformation in main structural members.

In this study, the applicability of the direct displacement design method [6] on an DTBF structure is investigated. The design procedure is applied to a single-degree-of-freedom (SDOF) system first, and is further extended to 3- and 5-story structures to verify the applicability of the method. The BRBs are

* Corresponding author. Tel.: +82-31-290-7563; fax: +82-31-290-7570.
E-mail address: jinkoo@yurim.skku.ac (J. Kim).

0141-0296/$ - see front matter © 2003 Published by Elsevier Ltd.
doi:10.1016/j.engstruct.2003.11.005

designed to resist lateral load so that the maximum roof displacement coincides with a given target displacement. The pin-connected beams and columns are designed for gravity loads plus the seismic load transferred from the braces so that they remain elastic during earthquake. Two artificial earthquake records are generated from an UBC 97-based design spectrum, and the response spectra constructed using the records are utilized in the design process. Time-history analyses are carried out to check whether the maximum displacements coincide with the target displacements.

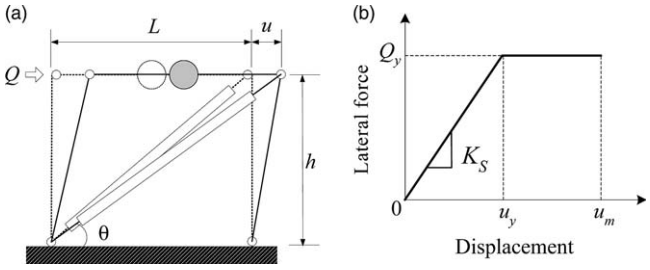

Fig. 2. Analysis model and load–displacement relationship of a single-story DTBF: (a) analysis model and (b) load–displacement relationship.

2. Design procedure for an SDOF system

2.1. Design procedure

Fig. 1 shows the schematic of an DTBF structure, in which the BRBs are designed to resist all lateral loads. The pin-connected beams and columns are designed for gravity load plus the member force transferred from brace, so that they remain elastic during the earthquake. It is intended that the maximum roof displacement is almost the same or a little less than a given target displacement. The yield displacement of the single story structure with an BRB (Fig. 2), u_y, is derived as follows:

$$u_y = \frac{\sigma_y l_b}{E\cos\theta} \tag{1}$$

where σ_y is the yield stress, l_b is the length, θ is the slope, and E is the elastic modulus of the brace. Note that the yield displacement does not depend on the cross-sectional area of the brace, but on the yield strength and geometry of the brace. This simplifies the design procedure, because the yield displacement is known before the size of the braces is actually determined. Once the target displacement of the structure, u_m, required to meet the performance objective is determined, the system ductility demand μ is obtained as follows:

$$\mu = u_m/u_y \tag{2}$$

Using the ductility demand, the effective damping ratio, β_{eff}, can be obtained as follows when the post-yield stiffness of the brace is assumed to be zero [5]:

$$\beta_{eff} = \beta + \beta_{eq} = \beta + \frac{2(\mu-1)}{\pi\mu} \tag{3}$$

where β is the inherent damping of the structure. Although 5% of the critical damping is usually used for inherent damping in seismic analysis of structures, the conventional practice may be questionable for hinge-connected frames in which only BRB yields and the other structural members remain elastic, especially when the hysteretic damping is accounted for separately. However, as no experimental data are available for such a structure system, 5% of critical damping was adapted in this study.

In the next step, the design spectrum is modified accommodating the effective damping, then it is transformed into a pseudo-acceleration–maximum displacement response spectrum (ADRS) format to obtain design load corresponding to a target displacement. The design spectrum for a specific equivalent damping ratio can be constructed from the 5% damping spectrum using the reduction factor provided in references such as ATC-40 [7] or FEMA-273 [8]. To convert a design spectrum with the standard S_a vs. T (period) format to ADRS format, it is necessary to determine the value of S_d for every point on the curve corresponding to each combination of S_a and T. This can be done using the following relation [7]:

$$S_d = (T^2/4\pi^2)S_a g \tag{4}$$

In this study, the ADRS diagram was derived from a response spectrum for artificial earthquake generated from a design spectrum to check whether the time-history analysis results for maximum displacements of the model structures, designed in accordance with the displacement-based design procedure, coincide well with the given target displacements. The acceleration corresponding to the target displacement, S_a, can be read from the ADRS as shown in Fig. 3. The design force is the acceleration multiplied by the mass of the structure,

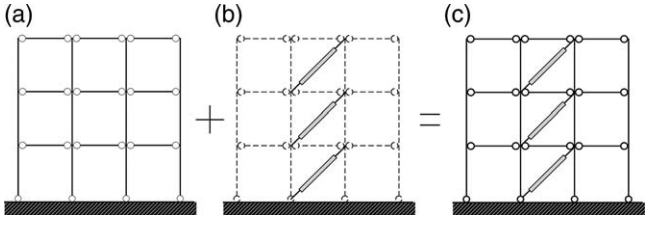

Fig. 1. Schematic of a damage-tolerant brace frame (DTBF) system: (a) main frame, (b) BRB and (c) DTBF.

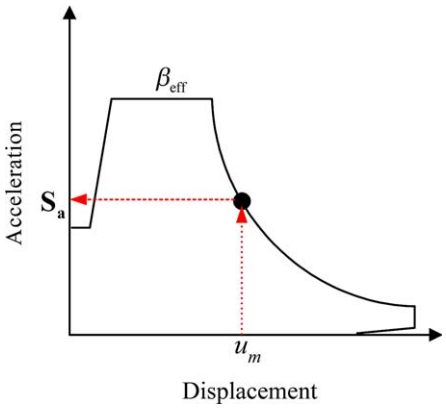

Fig. 3. Estimation of the maximum acceleration response.

m, as follows:

$$Q_y = mS_a \tag{5}$$

The cross-sectional area of BRB, A_b, satisfying the target performance point for a given seismic load is determined as follows:

$$A_b = \frac{Q_y l_b}{u_y E \cos^2\theta} = \frac{Q_y}{\sigma_y \cos\theta} \tag{6}$$

The lateral stiffness of the system, K_s, is obtained as follows as a function of cross-sectional area and the length of the brace:

$$K_s = \frac{A_b E}{l_b}\cos^2\theta \tag{7}$$

Fig. 2(b) depicts the force–displacement relationship of the system when the post-yield stiffness of BRB is zero.

2.2. Numerical example for an SDOF system

The above design procedure is applied to the SDOF system shown in Fig. 2(a). The following properties are assigned to the structure: weight = 100 kN, story height h= 4.0 m, width L= 6.0 m, column =H 250 × 250 × 9× 14 (mm), beam =H 420 × 200 × 8 × 13, and elastic modulus E= 210 GPa. The yield stress of the brace is assumed to be 100 MPa. The low-strength steel, which is currently available in Japan as an effective material for yield devices, is used in this study so that BRB start yielding while the other members remain elastic. The brace is assumed to show elastic–perfectly plastic behavior. The beam is pin-connected to the columns and the columns are pin-connected to the base so that lateral load is resisted mainly by the brace. The design spectrum with seismic coefficients C_a= 0.44 and C_v= 0.74, which is shown in Fig. 4(a) is used to generate an earthquake time-history record [9]. The design spectrum is recommended for seismic event of 2400 year return period in Korea [10]. The time history of the artificial record is plotted in

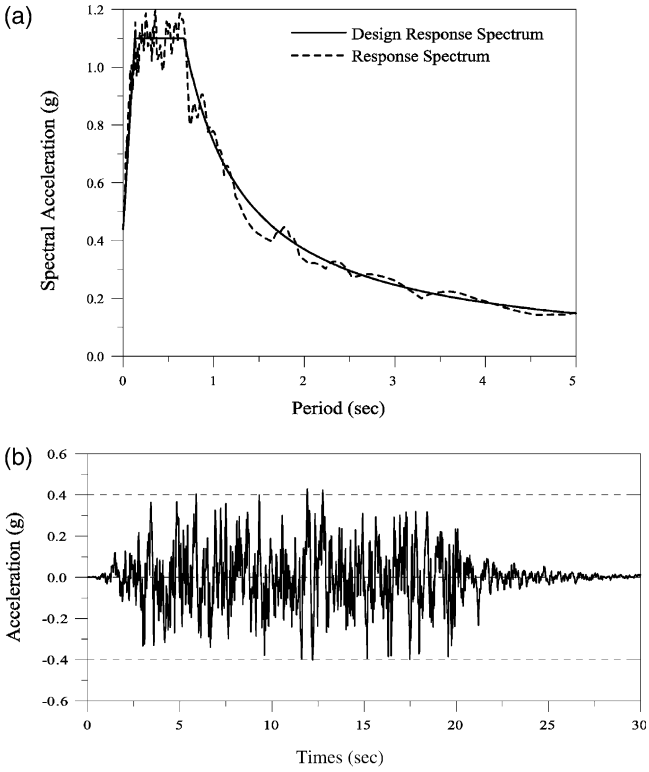

Fig. 4. Seismic load used in the analysis and design: (a) design spectrum and the response spectrum constructed from the artificial record and (b) time history of the artificial earthquake record.

Fig. 4(b). A response spectrum is constructed using the time-history record, which is depicted in Fig. 4(a) by the dotted curve, and is used in the design process. In the first step, the target displacement is set to be 1.5% of the structure height, which is 6 cm. The yield displacement obtained from Eq. (1) is 0.41 cm, and the ductility ratio becomes 14.6 when the structure deforms to the target displacement. With this ductility ratio, the effective damping ratio is computed to be 0.687. The response spectrum is modified considering the effective damping and is transformed to an acceleration–displacement diagram. In the diagram, the acceleration response corresponding to the target displacement turns out to be 0.17 g, and the yield force of 16.7 kN is obtained by multiplying the structure mass to the acceleration response. Finally, the required sectional area of the brace is computed using Eq. (5) as 2.0 cm^2. The nonlinear analysis program code DRAIN-2D+ [11] was used to analyze the structure. The maximum displacement of the structure obtained from time-history analysis using the generated artificial earthquake record turns out to be 5.7 cm, which is quite close to the target displacement of 6.0 cm.

3. Application to multi-story structures

The derivation of structural responses and design forces of a multi-story structure using an equivalent SDOF system is the key procedure in nonlinear static analysis and design methods, such as the capacity spectrum method or the direct displacement-based design. The nonlinear static procedures, however, have inherent limitations in their application. Krawinkler [12] pointed out that there is no physical principle that justifies the existence of a stable relationship between the hysteretic energy dissipation and the equivalent viscous damping, particularly for highly inelastic system. Fajfar [13] stated that pushover analysis is based on a very restrictive assumption, i.e. a time-independent displacement shape, and it is in principle inaccurate for structures where higher mode effects are significant. Nevertheless, the nonlinear static procedures are considered to be powerful alternative to nonlinear dynamic approach, particularly in preliminary analysis and design stage of regular, low-rise structures, for their simplicity in concept and convenience in application.

3.1. Design objectives

In multi-story structures, the objectives of seismic design for a given earthquake load are set as follows: (i) the maximum displacement is equal to the target displacement; (ii) the maximum inter-story drifts are the same in all stories; (iii) braces in all stories yield simultaneously in pushover analysis; and (iv) the energy dissipated in each story for unit cross-sectional area of the brace is the same. Among the design objectives, the third one can be achieved easily if the size of the braces in each story is determined proportionally to the seismic story shear force applied statically to the structure. Fig. 5(a) shows the distribution of seismic story force, which increases linearly with height, and the corresponding story displacement. Fig. 5(b) presents the story shear–story displacement relationships (pushover curves) of a multi-story damage-tolerant structure in which braces with zero post-yield stiffness are installed. If the braces are designed in accordance with the proposed procedure, the yield displacement of each story will be the same. In this case, it can be expected that structural damage caused by an earthquake is evenly distributed throughout the stories.

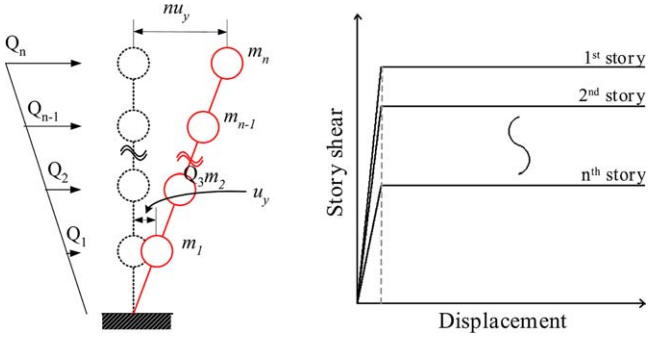

Fig. 5. Target deformation shape and pushover curve of a DTBF: (a) target deformation shape and (b) story shear vs. inter-story displacement.

3.2. Design procedure

The design process presented in the previous chapter for an SDOF structure can be further extended to multi-story structures as follows.

1. Computation of the maximum displacement at yield.

If the story heights and the yield strength of braces are the same throughout the structure, the maximum displacement at yield, u_y, is the story yield displacement, Eq. (1), multiplied by the number of stories, n:

$$u_y = \frac{\sigma_y l_b}{E\cos\theta} \times n \tag{8}$$

2. Computation of ductility demand.

The ductility demand is obtained by dividing the given target roof story displacement with yield displacement (Eq. (2)).

3. Transformation to an equivalent SDOF system.

A multi-story structure needs to be transformed to an equivalent SDOF structure to obtain design load. The yield displacement and maximum displacement of the equivalent SDOF system are obtained as follows [8]:

$$u'_y = \frac{u_y}{\Gamma}, \quad u'_m = \frac{u_m}{\Gamma} \tag{9}$$

where the modal participation factor for the fundamental mode, Γ, can be obtained as

$$\Gamma = \frac{\sum_{j=1}^{N} m_j \phi_j}{\sum_{j=1}^{N} m_j \phi_j^2} \tag{10}$$

where m_j is the mass of the jth story, and ϕ_j is the jth component of the fundamental mode shape vector. In this study, the mode shape is assumed to be a linear line as follows:

$$\phi = \left[1, \frac{n-1}{n}, \frac{n-2}{n}, \ldots, \frac{2}{n}, \frac{1}{n}\right] \tag{11}$$

where n is the number of stories. It is illustrated in the following section that the fundamental mode shape of a low-rise DTBF structure designed following the proposed procedure is close to a linear line. However, as the number of story increases, the assumption of linear mode shape is violated due to the deformability of the columns.

4. Estimation of effective damping (Eq. (3)) and determination of acceleration response, S_a, from the acceleration–displacement diagram.

5. Computation of design force.

The design base shear of the original multi-story structure can be obtained by multiplying the acceleration response of the equivalent SDOF structure obtained in the previous step to the effective mass for the fundamental mode:

$$F_{y1} = M^* S_a \tag{12}$$

where the effective modal mass, M^*, can be obtained as follows:

$$M^* = \frac{\left(\sum_{j=1}^{N} m_j \phi_j\right)^2}{\sum_{j=1}^{N} m_j \phi_j^2} \tag{13}$$

6. Estimation of the cross-sectional area of the brace in the first story.

The design force obtained from Eq. (12) corresponds to the base shear of the original structure, and the cross-sectional area of the brace in the first story is obtained as follows:

$$A_1 = \frac{F_{y1}}{\cos\theta \sigma_y} \tag{14}$$

Then the cross-sectional areas of braces in the other stories are determined proportionally to the story shear as follows:

$$A_1 \left[1, \frac{\sum_{x=2}^{n} Q_x}{\sum_{x=1}^{n} Q_x}, \frac{\sum_{x=3}^{n} Q_x}{\sum_{x=1}^{n} Q_x}, \ldots, \frac{\sum_{x=n-1}^{n} Q_x}{\sum_{x=1}^{n} Q_x}, \frac{\sum_{x=n}^{n} Q_x}{\sum_{x=1}^{n} Q_x}\right] \tag{15}$$

where A_1 is the cross-sectional area of the brace in the first story. The seismic story force in the xth story, Q_x, needs to be determined considering higher mode effects. In this study, the following equation from Korean seismic design code [14] is used to distribute the base shear throughout the stories:

$$Q_x = \frac{W_x h_x^k}{\sum_{i=1}^{n} W_i h_i^k} \times V \qquad \begin{bmatrix} T \le 1 \text{ s} & k = 1.0 \\ 1 < T \le 2 & k = 1.5 \\ T > 2 & k = 2.0 \end{bmatrix} \tag{16}$$

where V is the base shear, T is the fundamental natural period of the structure, h is the story height, and W_x is the weight of the xth story. It should be noted that the sizing of braces based on Eqs. (15) and (16) results in linear pushover deflected shape. However, for high-rise structures with the exponent k larger than 1.0, in which the story-wise distribution of acceleration response is nonlinear, the fundamental mode shape deviates from straight line due to deformability of columns. Therefore, the assumption of linear mode shape only applies to low-rise structures with k= 1.0.

7. Verification using time-history analysis.

The structure designed in accordance with the proposed procedure needs to be checked whether the design objectives are achieved for the given seismic load. As the pushover curve of the designed structure is the same with what is assumed in the design process, the maximum displacement computed from a nonlinear static analysis, such as the capacity spectrum analysis, will be identical to the target displacement. However, as the braces are distributed proportionally to the story shear based on the fundamental mode of vibration, the maximum displacement obtained from time-history analysis may be different from the target displacement.

4. Numerical example

4.1. Model structures and earthquake records

The design procedure presented above was applied to 3- and 5-story structures as shown in Fig. 6. The hinge-connected beams and columns were designed so that they remain elastic for gravity and lateral seismic load. The story weight of the structure is 100 kN. The selected members, expressed following the Korean Standard (KS), are presented in Table 1.

The earthquake record used previously for analysis of SDOF system (Fig. 4(b)) was used again to verify the validity of the design (this record is named as EQ-1). Another artificial record (EQ-2) was also generated based on the same design spectrum, and the

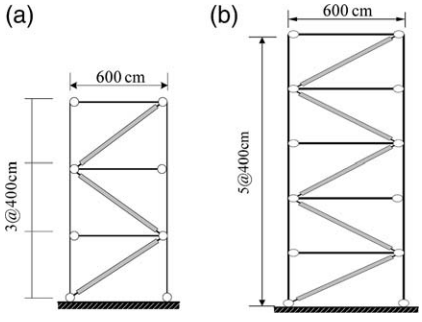

Fig. 6. Model structures for application of the proposed design procedure: (a) 3-story structure and (b) 5-story structure.

Table 1
Member size of model structures (unit: mm)

Story	Columns	Beams
(a) 3-Story		
1–2	H 250 × 250 × 9 × 14	H 400 × 200 × 8 × 13
3	H 200 × 200 × 8 × 12	
(b) 5-Story		
1–3	H 300 × 300 × 10 × 15	H 400 × 200 × 8 × 13
4–5	H 250 × 250 × 9 × 14	

response spectrum constructed using the time-history record EQ-2 turned out to coincide well with the design spectrum.

4.2. Design of braces

The cross-sectional areas of BRBs required to meet the given design objectives were determined for the four target top-story displacements: 1.0% (Case A), 1.5% (Case B), 2% (Case C), and 2.5% (Case D) of the structure height. The response spectra constructed using the artificial records EQ-1 and EQ-2 were used to design the braces. The sizes of the braces designed using the response spectrum corresponding to EQ-1 are presented in Table 2, and the fundamental periods of the structures designed for the four target displacements are given in Table 3. From the table, it can be noticed that the natural periods of braced frames with pin-connected beam–column joints are generally longer than those of rigid frames.

4.3. Pushover curves and mode shapes

Fig. 7 depicts the pushover curves of the 5-story model structure designed for target displacement of 1.0% of building height (Case A) for EQ-1. It can be observed that the story yield displacement of the 5-story structure is the same at each story, as intended in the design. Fig. 8 shows the mode shapes of the model structures designed for Case A. It can be observed that the mode shapes of the 3- and 5-story structures are close to linear lines.

Table 2
Cross-sectional area of braces (unit: cm^2)

Story	Case A	Case B	Case C	Case D
(a) 3-Story structure				
1	2.18	1.09	0.97	0.89
2	1.82	0.91	0.81	0.74
3	1.09	0.54	0.49	0.44
(b) 5-Storystructure				
1	2.53	1.72	1.31	1.01
2	2.35	1.60	1.22	0.94
3	2.02	1.38	1.05	0.81
4	1.52	1.03	0.79	0.61
5	0.83	0.57	0.43	0.33

Table 3
Fundamental periods of model structures designed for various target displacements

Model structure	Case A	Case B	Case C	Case D
3-Story	0.83	1.15	1.21	1.27
5-Story	1.10	1.33	1.52	1.72

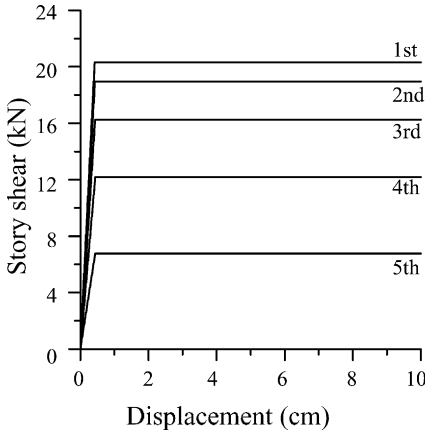

Fig. 7. Story force–story displacement relationships of the 5-story model structure.

4.4. Maximum displacements

Figs. 9 and 10 illustrate the maximum story displacements and inter-story drifts of the model structures computed from time-history analyses with the artificial earthquake record EQ-1. It can be observed that the maximum displacements correspond well with the target displacements in most cases. It can also be noticed that the maximum story displacement curves are close to linear lines, and the maximum inter-story drifts are relatively uniform as desired. Similar results were obtained from the analysis of the model structures designed for the earthquake record EQ-2, as can be observed in Fig. 11.

4.5. Column loads induced by lateral seismic load

Figs. 12 and 13 plot the maximum axial load and bending moment, respectively, obtained from time-history analysis of the structures designed for EQ-1. It can be observed that the axial force induced in columns due to the lateral load is less than 4% of the yield load,

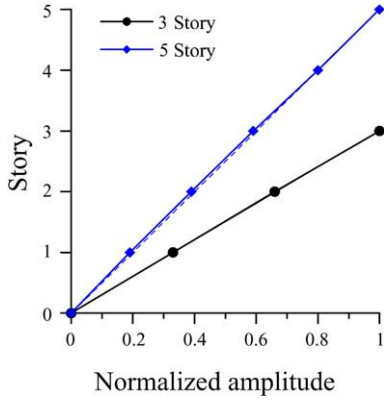

Fig. 8. Mode shapes of model structures.

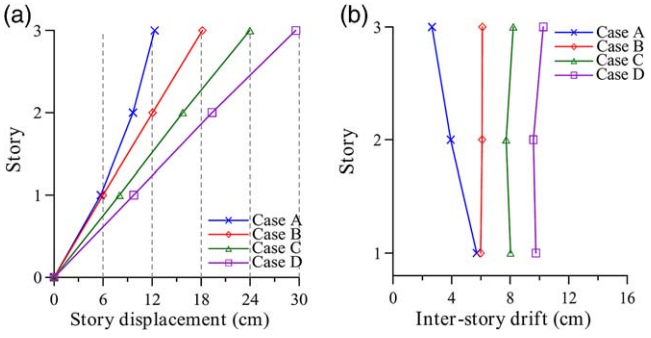

Fig. 9. Maximum displacements obtained from time-history analysis (3-story): (a) maximum story drifts and (b) maximum inter-story drifts.

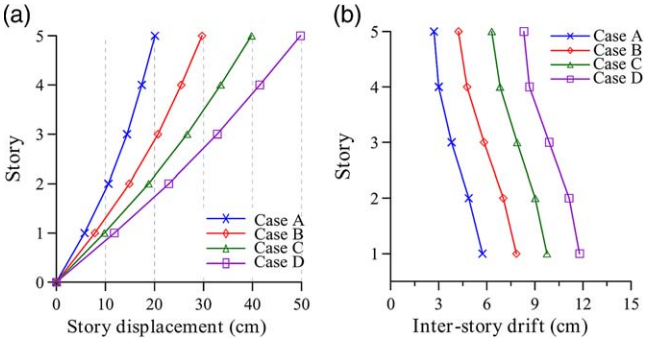

Fig. 10. Maximum displacements obtained from time-history analysis (5-story): (a) maximum story drifts and (b) maximum inter-story drifts.

which is small enough to be neglected. Also the column moments induced by lateral load are less than 15% of the yield moment in all target displacement cases.

4.6. Hysteretic energy dissipated by unit area of brace

Fig. 14 shows the hysteretic energy dissipated by the brace located in each story of the model structures,

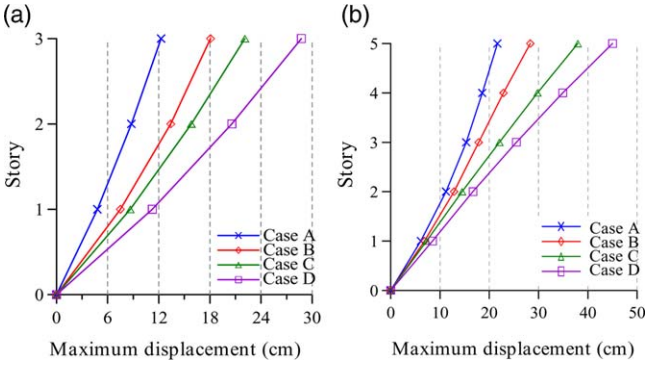

Fig. 11. Maximum displacements of model structures obtained from time-history analysis with earthquake record EQ-2: (a) 3-story and (b) 5-story.

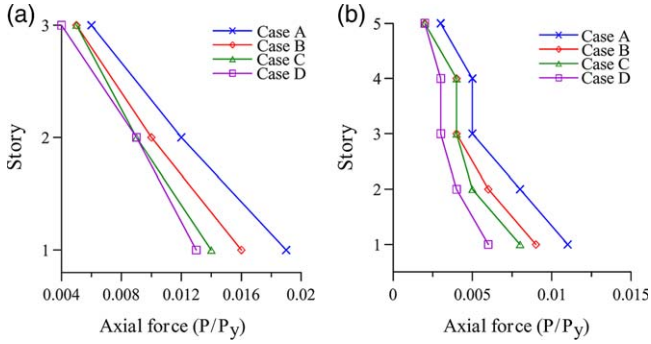

Fig. 12. Maximum column axial force in each story of the model structures: (a) 3-story and (b) 5-story.

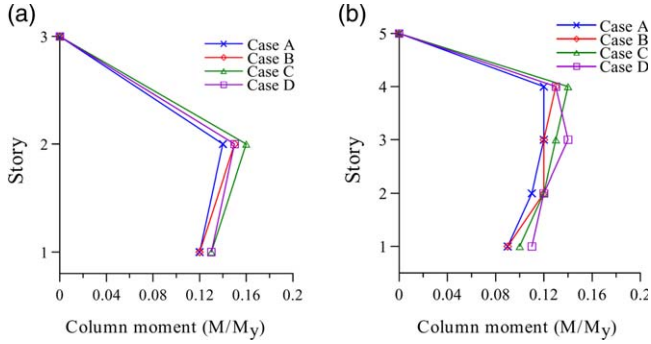

Fig. 13. Maximum column moment in each story of the model structures: (a) 3-story and (b) 5-story.

where it can be observed that the dissipated energy decreases as the structure height increases. However, the hysteretic energy dissipated per unit area of brace, illustrated in Fig. 15, shows that the dissipated energy per unit area is relatively uniformly distributed throughout the story.

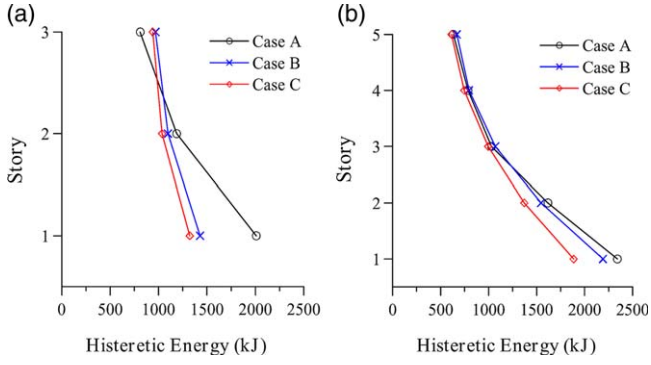

Fig. 14. Story-wise distribution of hysteretic energy: (a) 3-story and (b) 5-story.

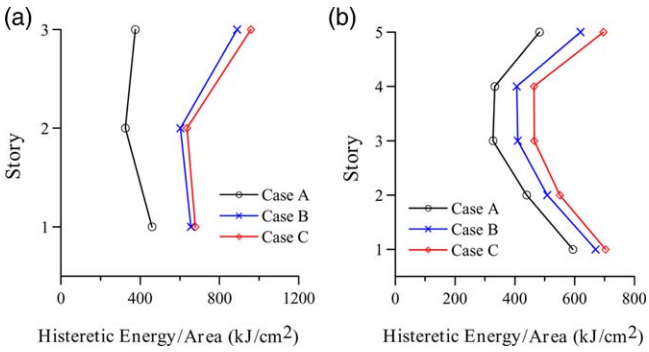

Fig. 15. Distribution of hysteretic energy per unit area of brace: (a) 3-story and (b) 5-story.

4.7. Effect of yield strength of brace on bending moment of columns

Fig. 16 plots the maximum bending moment induced in columns due to the seismic load when the BRB with yield stresses of 100 and 240 MPa are used to meet the target displacement of Case A (1.0% of the structure height, H) and Case B (1.5% H). It can be observed that the column bending moment in each story is larger when higher yield stress steel is used for the brace. Therefore, to conform to the basic principle of the DTBF systems, the use of low-strength steel for braces is preferable.

4.8. Ductility of buckling-restrained braces

According to time-history analysis results, the maximum brace ductility ratio for Case D reached up to 29 in 5-story structure, when computed assuming that full length of brace yielded. Since in BRBs, the yielding length is usually smaller than the full length of the brace, the actual values for the ductility ratio will be larger. According to experimental research of Iwata et al. [3], BRBs with yield stress of 262 MPa showed stable hysteretic behavior when they were stressed more than 3% of strain, which corresponds to ductility ratio of 24. Similar results were obtained by Black et al. [4], who showed that a structure with BRBs with yield stress around 280 MPa behaved stably at 3% of inter-story drift. The ductility ratio at this point reached 20. It also can be observed that cumulative ductility decreases with increasing peak ductility. Yamaguchi et al. [5] carried out experiments of half frames with BRBs made of low-strength steel (F_y= 96 MPa). Although not shown specifically in a table, it can be observed in the figure that the maximum ductility ratio reached as high as 30. Therefore, the basic assumption of this study that the brace behaves stably under ductility ratio lager than 30 needs to be validated by further experimental study.

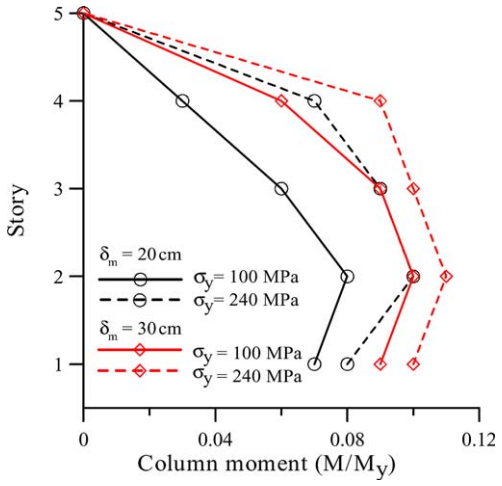

Fig. 16. Effect of yield stress of brace on maximum column moment.

5. Conclusions

In this study, a performance-based seismic design procedure was applied to buckling-restrained braced frames with pin-connected beam–column joints. The proposed design procedure assumes shear-type story displacement shape and the straight-line fundamental mode shape. The performance of model structures designed to meet a specified target displacement was evaluated by nonlinear time-history analysis to check whether the given performance objective was satisfied or not.

According to the numerical results, the maximum displacements of 3- and 5-story model structures designed in accordance with the presented procedure corresponded well with given target displacements. Therefore, it can be concluded that the proposed design procedure can be a convenient tool for performance-based seismic design of a low-rise structure with BRBs. The analysis results also verified that the axial forces and bending moments induced in columns of low-rise structures were not significant, which implies that the philosophy of the damage-tolerant structure can be realized in such structures; i.e. the BRBs dissipate most of the vibration energy through inelastic deformation while the other structural members remain elastic and undamaged. It should be pointed out, however, that the maximum ductility ratio of BRB larger than 30, observed in the design for target drift ratio of 2.5%, needs to be validated by further experimental study.

Acknowledgements

This research is funded by the Korea Science and Engineering Foundation under Grant No. R01-2002-

000-00025-0. This financial support is gratefully acknowledged.

References

[1] Wada A, Connor JJ, Kawai H, Iwata M, Watanabe, A. Damage tolerant structures. Fifth US–Japan Workshop on the Improvement of Building Structural Design and Construction, Practices, 1992.

[2] Saeki E, Maeda Y, Nakamura H, Midorikawa M, Wada A. Experimental study on practical-scale unbonded braces. J Struct Constr Eng AIJ 1995;476:149–58.

[3] Iwata M, Kato T, Wada A. Buckling-restrained braces as hysteretic dampers. Proceeding of Behavior of Steel Structures in Seismic Areas. Rotterdam: Balkema; 2000.

[4] Black C, Makris N, Aiken I. Component testing, stability analysis and characterization of buckling restrained braces. Final Report to Nippon Steel Corporation, Japan, 2002.

[5] Yamaguchi M, et al. Earthquake resistant performance of moment resistant steel frames with damper. Proceeding of Behavior of Steel Structures in Seismic Areas. Rotterdam: Balkema; 2000.

[6] SEAOC. Tentative guidelines for performance based seismic engineering. SEAOC Blue Book. Structural Engineers Association of California; 1999.

[7] ATC, Applied Technology Council. Seismic evaluation and retrofit of concrete buildings. ATC-40, Redwood City, CA, 1996.

[8] FEMA. NEHRP Guidelines for the seismic rehabilitation of buildings. FEMA-273, Federal Emergency Management Agency, Washington, DC, 1997.

[9] Vanmarcke EH, Gasparini DA. A program for artificial motion generation, user's manual and documentation. Department of Civil Engineering, Massachusetts Institute of Technology, 1976.

[10] Korea Institute of Earthquake Engineering. Report on performance-based seismic design provision, 1997.

[11] Tsai KC, Li JW. DRAIN-2D+, a general purpose computer program for static and dynamic analyses of inelastic 2D structures supplemented with a graphic processor. Report No. CEER/R86-07, National Taiwan University, Taipei, Taiwan, 1997.

[12] Krawinkler H. New trends in seismic design methodology. Proceeding the Tenth European Conference on Earthquake Engineering, Vienna 1994.

[13] Fajfar P. A nonlinear analysis method for performance-based seismic design. Earthquake Spectra 2000;16(3):573–92.

[14] Architectural Institute of Korea. Regulations for building design loads, 2000.